Fermi National Accelerator Laboratory

FERMILAB-Pub-90/150

Optical Attenuation Length Measurements of Scintillating Fibers *

N. A. Amos, A. D. Bross and M. C. Lundin
Fermi National Accelerator Laboratory
P.O. Box 500
Batavia, Illinois 60510

July 14, 1990

* Submitted to Nucl. Instrum. Methods A.

Optical Attenuation Length Measurements of Scintillating Fibers

N.A. Amos, A.D. Bross, and M.C. Lundin
Particle Detector Group
Fermi National Accelerator Laboratory
Batavia, IL 60510

July 14, 1990

Abstract

We present data on optical attenuation length measurements of plastic scintillating fiber and show how the photodetector response as a function of wavelength can affect these measurements. In addition, we show that light propagation in stepped-index optical fiber is characterized by two distinct components.

Submitted to *Nuclear Instruments and Methods*

1 Introduction

Plastic scintillating fiber is being applied to many new detector applications for high energy physics. Calorimetry, tracking devices, and time-of-flight detectors have been built or are proposed to be built with scintillating fiber. The fiber performance can be characterized by the scintillator's intrinsic properties, light yield and fluorescence decay time, and by the light attenuation as a function of distance traveled in the fiber. We have constructed a simple system that uses UV excitation to excite fluorescence in the fiber, and we then measured its intensity as a function of position. Since the fluorescence distribution of light exiting a fiber is a function of the distance between the excitation source and the photodetector measuring the light, we used a number of different detectors in our study in order to show how the detector response can affect the attenuation length measurements. We also show that light reflected at the core-cladding interface and propagating down the fiber has a very different attenuation length from light that is reflected at the cladding-air interface.

2 Experimental Setup

2.1 Fiber Measurement System

The system we used to perform controlled studies on scintillating fiber consisted of three parts. The first component is a system of opposing pinch wheels that is used to position the fiber. One of the wheels is connected to a ten turn precision potentiometer which is powered by a constant voltage source. The fiber is then manually pulled through the wheels in order to make the measurements. In doing so, it turns the pinch wheels and the slider contact of the potentiometer. The slider contact thus provides a voltage that is proportional to the distance the fiber has been pulled through the wheels. With this system, 1 cm position accuracy is easily obtained. As the fiber is moved, it is excited by UV light from a low pressure mercury lamp. This light is piped from the lamp to the fiber excitation block (Figure 1) by a quartz fiber bundle. The measurements were always started at the far end of the fiber as referenced from the photodetector. This corresponded to a 5 meter excitation-source to detector distance. A large loop in the fiber between

the detector and the excitation block was taken up as the fiber was pulled through the pinch wheels, thus decreasing the excitation-source to detector distance. Throughout the measurements, the end of the fiber coupled to the photodetector remained fixed with respect to the photodetector.

The second part of the system was the photodetector itself. It was coupled directly to a Keithley model 480 picoammeter. The picoammeter provided a voltage proportional to the DC current provided by the photodetector. The last part of the system consisted of a set of buffer preamplifiers for the voltages from the potentiometer and the picoammeter. The preamplifier signals were digitized by an Ortec model AD811 ADC and readout via CAMAC into an AST 386 personal computer.

Four photodetectors were chosen for this study. They are the following:

1. United Detector Technologies model 221 one centimeter diameter silicon photodiode. Its response extends from 350 nm to 1100 nm.

2. Hamamatsu photomultiplier tube (PMT) type 6199. This PMT is characterised by a S-11 type response and is considered to be a general purpose PMT. Its range extends from 300-650 nm. The photocathode material is Cesium-Antimony and the tube has a borosilicate glass window;

3. Thorn EMI (PMT) type 9902B. This PMT is characterized by a bialkali spectral response extending from 350 nm to approximately 600 nm. The photocathode material is also Cesium-Antimony and the tube has a borosilicate glass window;

4. Hamamatsu (PMT) type 669. This PMT has an extended red multialkali photocathode. Its range extends from 300-900 nm. The tube has a borosilicate glass window.

The relative quantum efficiency versus wavelength for these four detectors in the wavelength region between 400 and 680 nm is given in Figure 2.

In order to make wavelength corrected comparisons among the different detectors, the spectral response of each detector under study was required to be known, and the fluorescence distribution of light exiting a fiber as a function of the distance between the excitation point and the detector end of the fiber needed to be measured. The system used for these fluorescence measurements is shown in Figure 3. For each fiber that was measured using the

four photodetectors listed above, one series of measurements was performed using this system. The system shown in Figure 3 consists of an ISA model HR 320 monochrometer coupled to a Princeton Instrument's IRY700 intensified diode array detector head. The IRY700 uses a micro-channel plate intensifier that has a S-20 photocathode. With a 147 groove/mm grating, this system gave approximately 0.5 nm resolution/diode. Measurements were taken with this system in the same way as was performed with the other photodetectors. In all cases, the fiber positioning mechanism described above was used. However, in measurements using the monochrometer, the light from the fiber was coupled into the entrance optics of the monochrometer with a spherical lens. This arrangement more closely matched the numerical aperture of the fiber to that of the monochrometer. The monochrometer data are corrected for the wavelength dependent throughput of the monochrometer and also for any non-uniformity of response due to the wavelength dependent quantum efficiency of the IRY700. Therefore, data obtained with this system are proportional to the true number of photons/wavelength bin exiting the fiber. Changes, as a function of excitation-source to detector distance, in the fluorescence distribution of scintillation light exiting the fiber can then be accurately determined.

2.2 Fiber Preparation

In making these measurements, the preparation of the end of the fiber that was coupled to the photodetector (or monochrometer) was extremely important. Each test fiber had one end epoxied into a ferrule that could then be mounted in a positioning fixture (Figure 4). This procedure performed two important tasks. First, it allowed for precise and reproducible coupling of the fiber to the photodetector. Secondly, it stopped propagation in the fiber of light that is reflected at the cladding-air interface.

There are two distinct components to the light that can be transmitted in a stepped-index optical fiber, (see Figure 5.) The first component, "core light," consists of those rays that are total internally reflected at the core-cladding interface. The second component, "cladding light," is light that is total internally reflected at the cladding-air interface. The attenuation properties of these two components are vastly different and must be taken into consideration when discussing the properties of this type of optical fiber. This will be described in detail in Section 3.

2.3 Measurements

A systematic series of attenuation and fluorescence measurements were completed on three different 1mm diameter fiber samples: Kyowa SCSF 81 [2], Kyowa 3-hydroxyflavone (3-HF) doped fiber, and a fiber fabricated at Fermilab that used 3-HF and rubrene as dopants. All of these fibers have a core material of polystyrene scintillator and a cladding of acrylic. Attenuation length measurements were made using the setup and procedures discussed in Section 2. These data obviously give the total signal, i.e., the signal integrated over all wavelengths in which the detector is sensitive. Each fiber was measured with the four photodetectors. Data were taken every 10 cm out to a distance of 1 meter from the detector and then every 20 cm out to a maximum distance of 5 meters. Typical attenuation length data, signal versus position, are shown in Figures 6-8. The solid lines represent fits to the data, (see Section 3.2.) A set of monochrometer measurements was also performed for each of these fibers. These data are shown in Figures 9-11. Measurements were taken at the same distances as for the PMT's and the photodiode, but, for clarity, only the data for 0.1, 0.2, 0.3, 0.4, 1, 2, 3, 4, and 5 meters are shown. These data demonstrate that the spectral distribution of scintillation light exiting the fiber changes as the excitation-source to detector position is increased. Light attenuation is a function of wavelength.

3 Results

3.1 Attenuation lengths - Core vs. Cladding light

As was described in Section 2, there are two components to the light that propagates along an optical fiber: core light and cladding light. Core light experiences total internal reflection at the core-cladding interface and has an attenuation length that is determined by absorption in the bulk and by the effective reflection coefficient at this interface. Small imperfections in the waveguide structure of the fiber will prevent this reflection coefficient from being 1. However, since the core-cladding interface is well controlled, this reflection coefficient can be very close to unity. A long attenuation length is then possible for this light. Cladding light consists of rays which are beyond the angle for total internal reflection at the core-cladding interface but can be trapped at the cladding-air interface (Figure 5). Since this external

interface cannot be well controlled, dust, scratches, fingerprints, etc. can significantly degrade the effective reflection coefficient for this light and thus its attenuation properties. Light propagation is then described as the sum of these two components, each with its own attenuation length.[1]

In order to have some degree of control over the cladding-air interface during the study of the separate core and cladding light components, the measurements were performed using a procedure similar to the one described in Reference 1. The pinch wheel system was not used in these measurements. Instead, a straight 2 meter section of fiber was mounted on an optical rail (see Figure 12) and the UV excitation block was simply moved along the fiber, and the source to detector position was recorded for each measurement. The detector end of the fiber was glued with 5 minute epoxy into a 2.5 cm diameter by 1 cm thick polystyrene disk. In this way the cladding light is coupled into the polystyrene disk and at the PMT faceplate is physically separated from the light exiting the core. A suitable mask was then used to select either the core or the cladding light for measurement.

Three measurements were taken: core light only, cladding light only, and total light. Data showing the different attenuation lengths from measurements on a 0.75 mm diameter fiber are given in Figure 13. As can be seen from this figure, the difference in the attenuation lengths can be quite large. At distances less than 30 cm, the cladding light actually dominates the signal. The points at "zero distance" were obtained by extrapolating from the last two measured points, those at distances of 1.7 and 3.5 cm. The measured ratio of cladding light to core light at the point of excitation is then approximately 4.1. This agrees well with what one would calculate considering only on axis rays in the fiber. For this calculation, we have used indices of refraction for polystyrene and acrylic at the peak of the scintillator's fluorescence emission, $\lambda_p = 420$ nm. We have (see Figure 5):

$$sin\theta_c^{co} = \frac{1.5}{1.62} \Rightarrow \theta_c^{co} = 68°$$

$$sin\theta_c^{cl} = \frac{1.0}{1.50} \Rightarrow \theta_c^{cl} = 42°$$

and

$$sin\hat{\theta}_c^{cl} = \frac{1.0}{1.62} \Rightarrow \hat{\theta}_c^{cl} = 38°$$

where θ_c^{co} is the critical angle at the core-cladding interface, θ_c^{cl} the critical angle at the cladding-air interface, and $\hat{\theta}_c^{cl}$ the angle in the core for light trapped at the cladding-air critical angle.

The ratio of the amount of light trapped at the cladding-air interface to the amount trapped in the core is then:

$$R = \frac{\int_{90-68}^{90-38} sin\theta d\theta}{\int_{0}^{90-68} sin\theta d\theta} \approx 4.4.$$

This is in good agreement with our data's extrapolation to zero distance.

3.2 Attenuation lengths - Photodetector Effects

For all the measurements described in this section, a ferrule was used with the fiber so that only attenuation of core light was considered. All attenuation length data were fit to single exponentials in two regions, 0 to 1 meter and 1 to 5 meters. All fitting was performed using the CERN package MINUIT. The errors on individual points are proportional to the square root of the value of each point such that the χ^2/DOF is unity. Table one shows the results for the three test fibers using the four photodetectors. The top and bottom numbers for each measurement correspond to the attenuation lengths (1/e point in meters) obtained for the 0 to 1 meter region and the 1 to 5 meter region, respectively. Figures 6-8 show data from measurements using the Hamamatsu 6199 PMT. The solid lines are the fits to the data.

Table 1: Attenuation Lengths (in meters)
(Bottom Value: 0-1 meter fit, Top Value: 1-5 meter fit)

	Fiber		
Detector	Kyowa SCSF 81	Kyowa 3-HF	Rubrene
Silicon Photodiode	1.2 ± 0.1	3.5 ± 0.2	1.1 ± 0.1
	3.1 ± 0.1	6.2 ± 0.2	2.5 ± 0.2
Thorn EMI 9902B	0.9 ± 0.1	2.5 ± 0.2	0.9 ± 0.1
	2.5 ± 0.1	5.7 ± 0.2	1.8 ± 0.1
Hamamatsu 6199	0.9 ± 0.1	3.0 ± 0.1	0.8 ± 0.1
	2.5 ± 0.1	6.0 ± 0.2	1.8 ± 0.1
Hamamatsu 669	1.0 ± 0.1	3.1 ± 0.2	1.0 ± 0.1
	3.3 ± 0.1	5.8 ± 0.2	2.3 ± 0.1

There are a number of relatively large differences in the measured attenuation lengths between the various detectors. These differences can be attributed to the different spectral responses of the four photodetectors and to the fact that attenuation in the fiber is a function of wavelength. In order to verify this, we used the monochrometer data and the wavelength dependent quantum efficiencies provided with each detector. For each fiber, an attenuation plot was generated for a given photodetector. This was performed in the following manner: Since the monochrometer data represent true "photon" attenuation, the "signal" attenuation, as measured by any detector can be reproduced by weighting the monochrometer data at each source position by the spectral response curve for a given detector and then summing over all wavelength bins to obtain the "simulated signal" at each point. A typical plot is shown in Figure 14 for the case of the SCSF 81 fiber and the Hamamatsu 6199 PMT readout. The points are the "simulated" data and the solid lines are the fits. The fitting was performed as described above. This calculation was performed for all combinations of fiber and photodetector, and the results are tabulated in Table 2.

Table 2: Simulated Attenuation Lengths (meters)
(Bottom Value: 0-1 meter fit, Top Value: 1-5 meter fit)

	Fiber		
Detector	Kyowa SCSF 81	Kyowa 3-HF	Rubrene
Silicon Photodiode	1.2 ± 0.1	3.7 ± 0.3	1.1 ± 0.2
	2.7 ± 0.1	6.2 ± 0.2	2.6 ± 0.1
Thorn 9902B	0.9 ± 0.1	2.6 ± 0.2	0.9 ± 0.1
	2.3 ± 0.1	5.7 ± 0.2	1.8 ± 0.1
Hamamatsu 6199	0.9 ± 0.1	2.9 ± 0.2	0.8 ± 0.1
	2.5 ± 0.1	5.9 ± 0.2	1.9 ± 0.1
Hamamatsu 669	1.0 ± 0.1	3.1 ± 0.3	1.0 ± 0.2
	2.7 ± 0.1	5.8 ± 0.2	2.3 ± 0.1

Tables 1 and 2 show that the "simulated' attenuation data reproduce the data taken with the actual photodetectors reasonably well.

In addition to fitting the data in two separate regions to single exponentials, we also fit some of the data to the form:

$$Y(X) = A_0 e^{-\frac{X}{\lambda_0}} + A_1 e^{-\frac{X}{\lambda_1}}$$

where Y is the signal, X is the UV source to detector distance, A_0 and A_1 are constants, and λ_0 and λ_1 are attenuation lengths. Figures 15 and 16 show fits of this form to the actual and "simulated' attenuation data for the Kyowa SCSF 81 fiber with the Hamamatsu 6199 PMT detector. This functional form fits the data quite well. One can then generate a "running attenution length" by dividing the function, Y(X), by the derivative of Y(X) with respect to X for values of X., i.e., we define the "running attenuation length" to be:

$$A_r(X) = \frac{Y}{\frac{dY}{dX}}.$$

The results of this calculation for the data shown in Figures 15 and 16 are given in Figure 17. The attenuation lengths determined by this procedure calculated at 0.5 meters and 3.0 meters agree well with the numbers obtained

for the 0 to 1 meter and 1 to 5 meter single exponential fits for this fiber.

A full mathematical treatment of the attenuation effects in plastic scintillating fiber would have to consider attenuation parameters that are a function of wavelength, both for losses due to bulk absorption and for reflection losses. This will be addressed in a future paper.

4 Summary

We have shown in a systematic fashion that detector response can influence attenuation length measurements for plastic scintillating fibers. Since what is really measured is "signal" attenuation, detectors with different spectral responses will give differing results. Valid comparisons of attenuation length measurements must first correct for the detector response so that real differences in the wavequide properties of the fiber(s) can be determined. It is also clear that only "core" light should be considered when evaluating the transmission properties of plastic scintillating fiber. Comparisons must also be made at similar excitation-source to detector distances, since the attenuation length is a function of this distance.

5 Acknowledgements

We would like to acknowledge the valuable assistance of Anna Pla and Kerry Mellott in the preparation of some of the fiber samples. This work was supported by the United States Department of Energy.

References

[1] C.M. Hawkes et. al., Decay Time and Light Yield Measurements for Plastic Scintillating Fibers, Nuclear Instruments and Methods in Physics Research, **A292** (1990) 329-336.

[2] Kyowa Gas Company, Tokyo, Japan.

Figure Captions

Figure 1. Diagram of the apparatus used for the attenuation length measurements.

Figure 2. Relative quantum efficiency curves for the four photodetectors.

Figure 3. Schematic diagram of the monochrometer system.

Figure 4. Fiber, ferrule, and positioner arrangement. (A): Arrangement used with the photodiode or PMT readout, (B): Arrangement used with the monochrometer system.

Figure 5. Ray diagram for rays at the core-cladding critical angle and at the cladding-air critical angle (see text.)

Figure 6. Fluorescence distributions versus excitation source position for the SCSF 81 fiber.

Figure 7. Fluorescence distributions versus excitation source position for the Kyowa 3-HF fiber.

Figure 8. Fluorescence distributions versus excitation source position for the fiber produced at Fermilab (3-HF + Rubrene doping).

Figure 9. Attenuation length data for the SCSF 81 fiber using the Hamamatsu 6199 PMT. The solid lines represent the fits to the data.

Figure 10. Attenuation length data for the Kyowa 3-HF fiber using the Hamamatsu 6199 PMT. The solid lines represent the fits to the data

Figure 11. Attenuation length data for the Rubrene fiber using the Hamamatsu 6199 PMT. The solid lines represent the fits to the data

Figure 12. Setup for measuring core-cladding light effects.

Figure 13. Attenuation length curves for "core," "cladding," and "core + cladding" light.

Figure 14. Simulated attenuation length data compiled from monochrometer data for the SCSF 81 fiber. This simulation is for the Hamamatsu 6199 PMT. The solid lines represent the fits to the data

Figure 15. Two exponential fit to data for the SCSF 81 fiber and using the Hamamatsu 6199 PMT as the photodetector.

Figure 16. Two exponential fit to simulated Hamamatsu 6199 PMT data for the SCSF 81 fiber.

Figure 17. "Running attenuation length" data for the fits shown in Figures 16 and 17. The top curve is for the simulated data and the bottom curve is for the data actually taken with the Hamamatsu 6199 PMT.

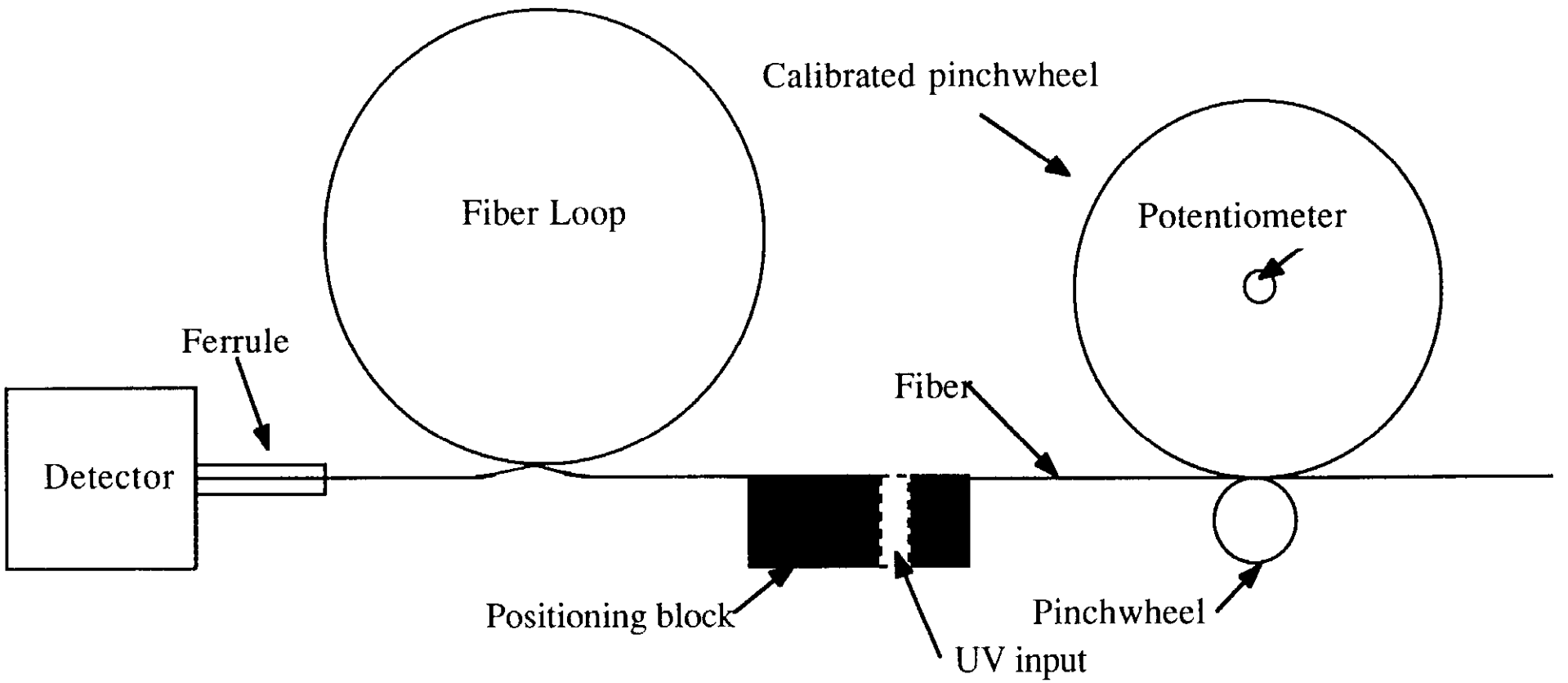
Calibrated pinchwheel
Fiber Loop
Potentiometer
Ferrule
Fiber
Detector
Positioning block
Pinchwheel
UV input

Figure 1

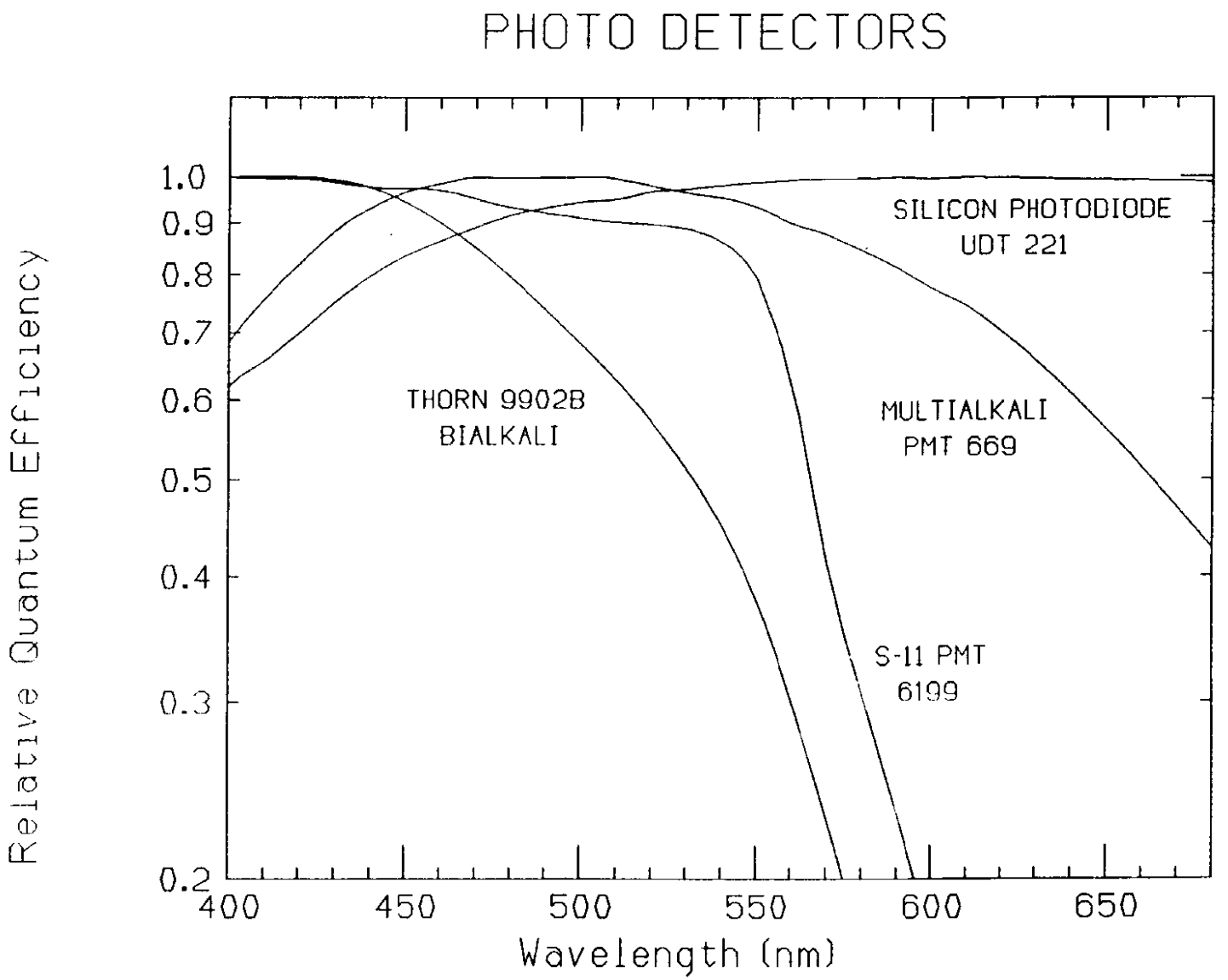
PHOTO DETECTORS
Relative Quantum Efficiency
1.0
0.9
0.8
0.7
0.6
0.5
0.4
0.3
0.2
400
450
500
550
600
650
Wavelength (nm)
SILICON PHOTODIODE
UDT 221
THORN 9902B
BIALKALI
MULTIALKALI
PMT 669
S-11 PMT
6199

Figure 2

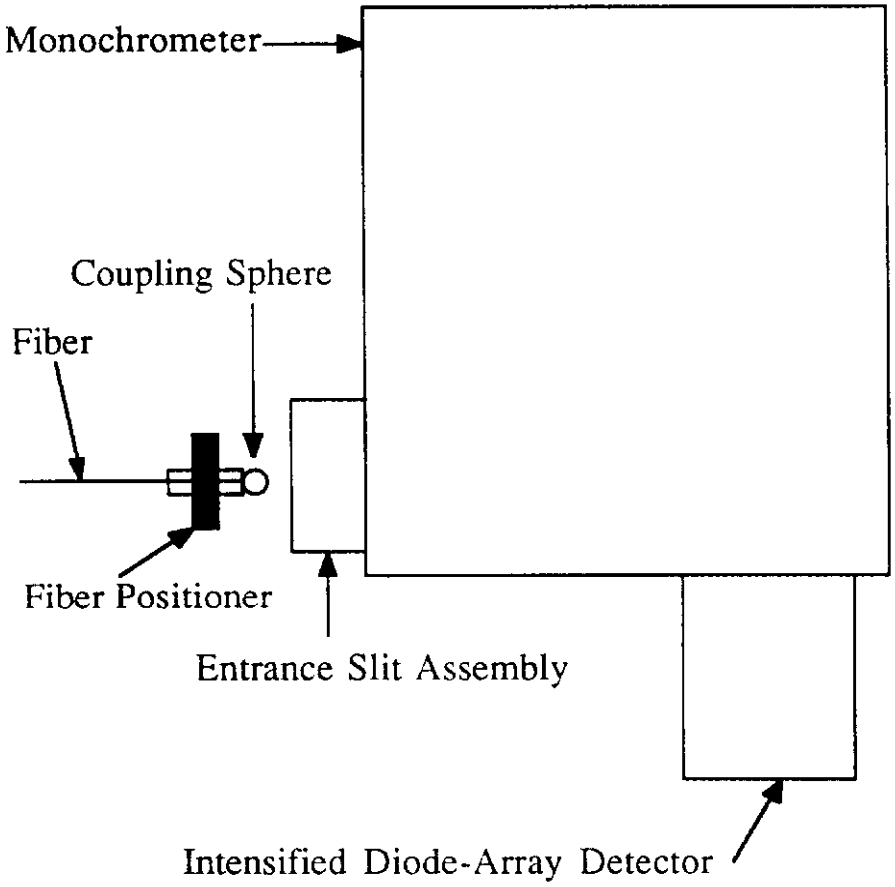
Monochrometer
Coupling Sphere
Fiber
Fiber Positioner
Entrance Slit Assembly
Intensified Diode-Array Detector

Figure 3

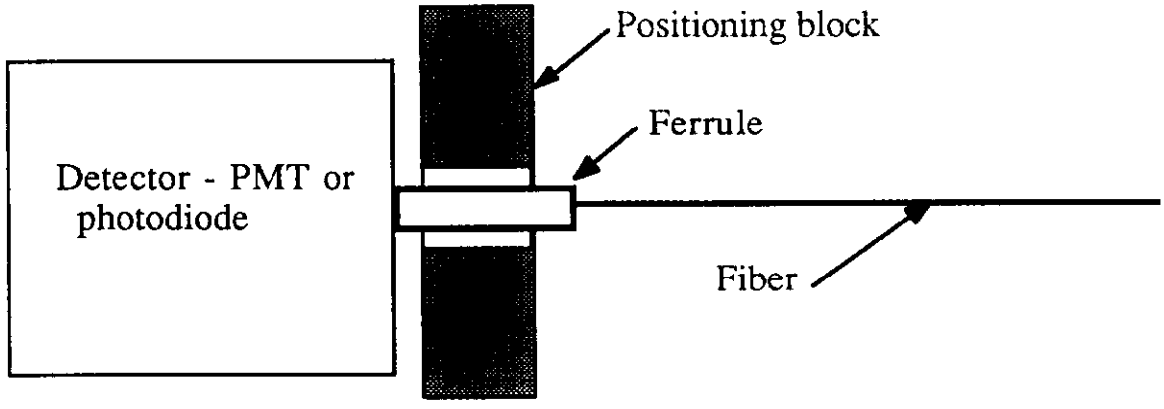
Positioning block
Ferrule
Detector - PMT or photodiode
Fiber

(A)

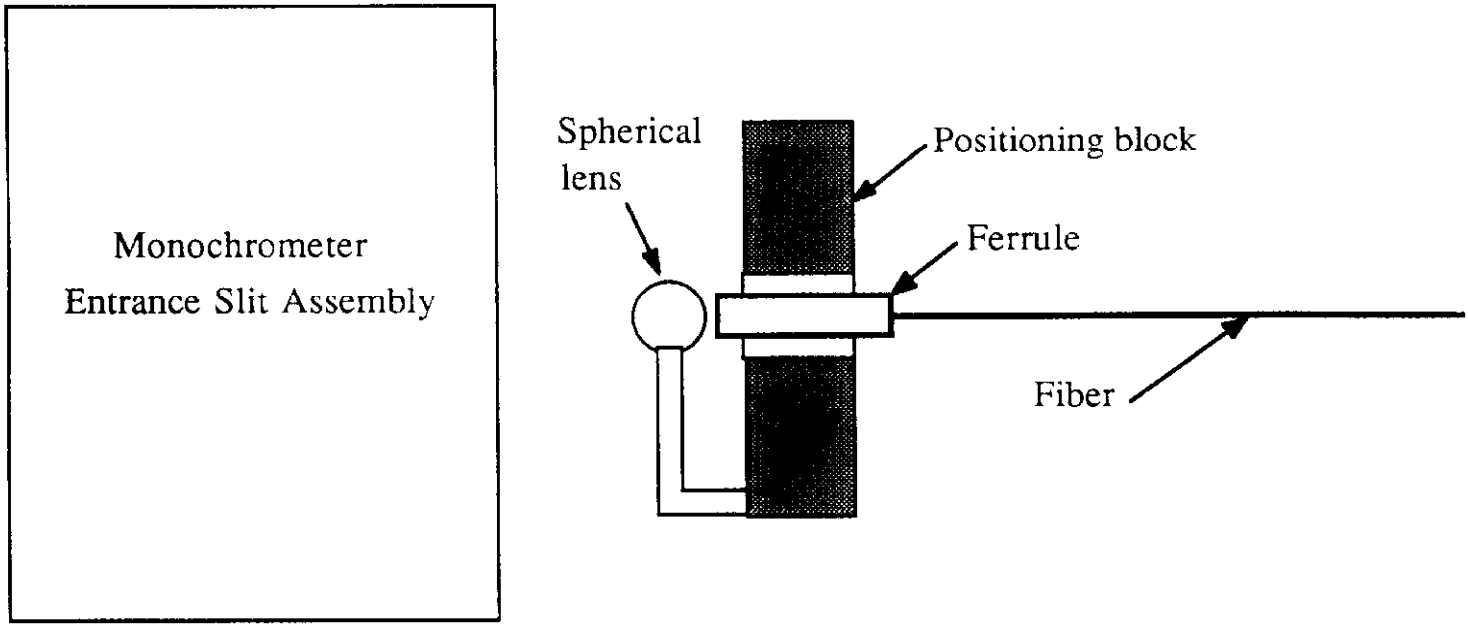
Monochrometer
Entrance Slit Assembly
Spherical lens
Positioning block
Ferrule
Fiber

(B)

Figure 4

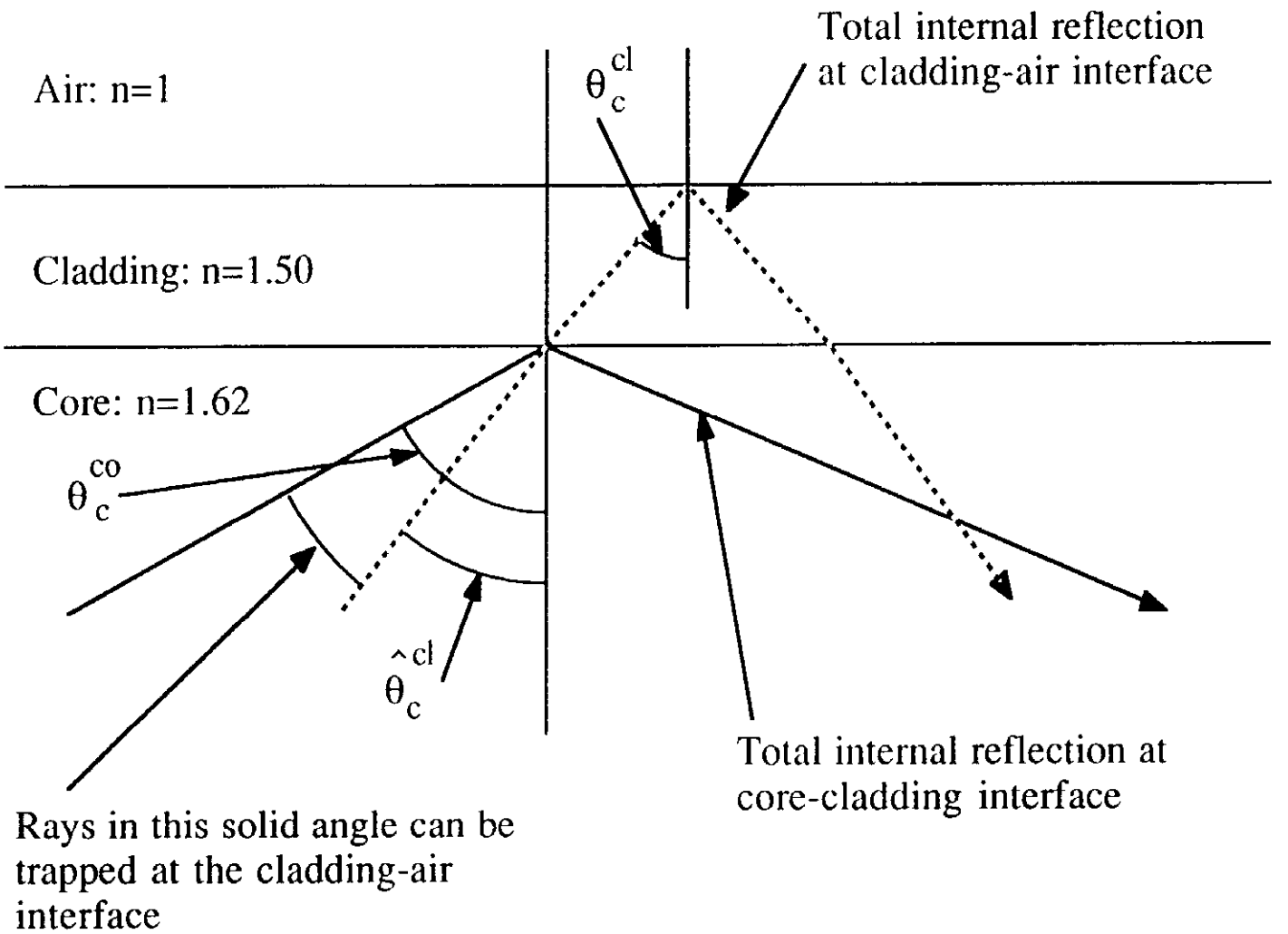
Air: n=1
Cladding: n=1.50
Core: n=1.62
θ_c^{cl}
Total internal reflection at cladding-air interface
θ_c^{co}
$\hat{\theta}_c^{cl}$
Total internal reflection at core-cladding interface
Rays in this solid angle can be trapped at the cladding-air interface

Figure 5

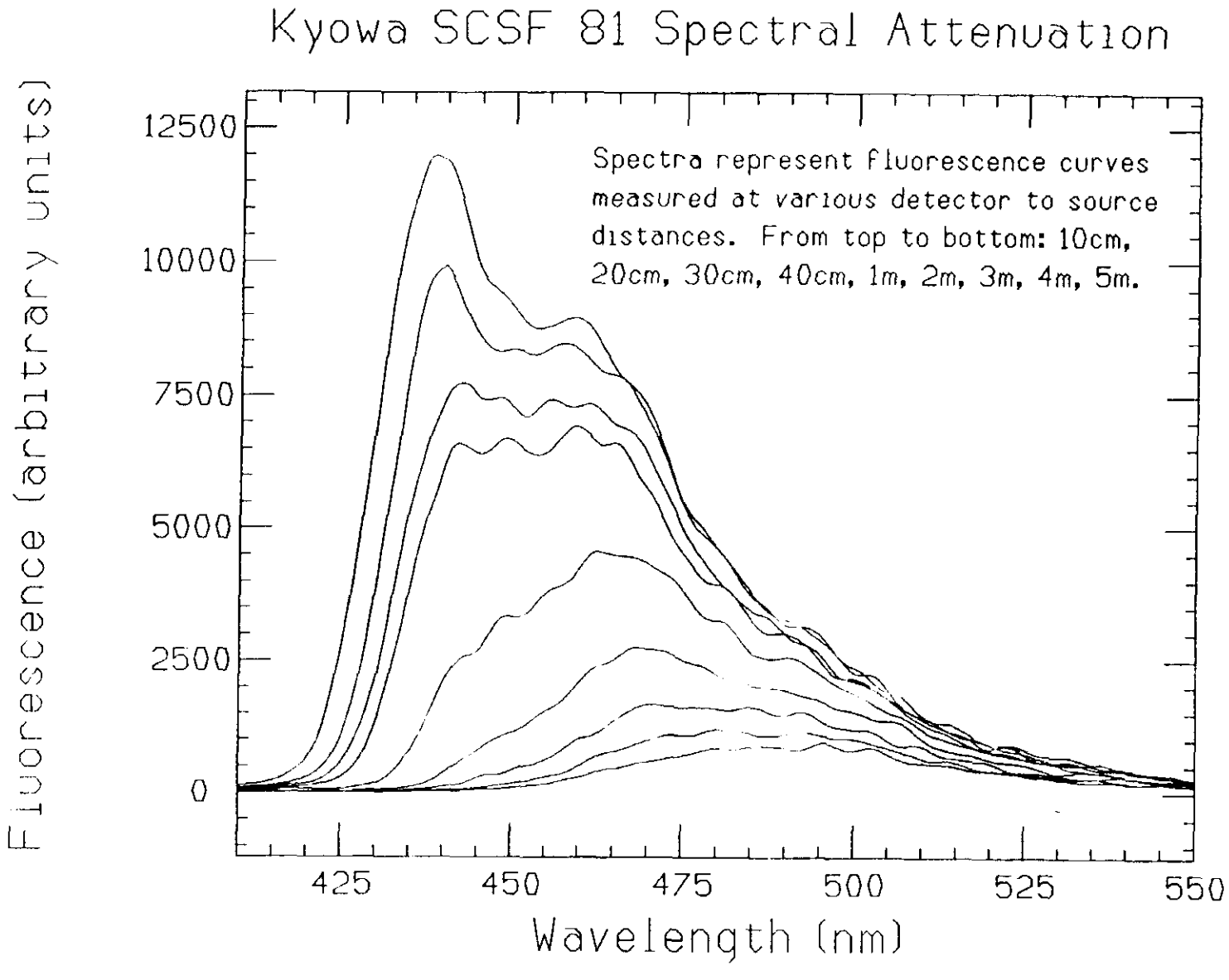
Kyowa SCSF 81 Spectral Attenuation
Fluorescence (arbitrary units)
12500
10000
7500
5000
2500
0
425
450
475
500
525
550
Wavelength (nm)
Spectra represent fluorescence curves measured at various detector to source distances. From top to bottom: 10cm, 20cm, 30cm, 40cm, 1m, 2m, 3m, 4m, 5m.

Figure 6

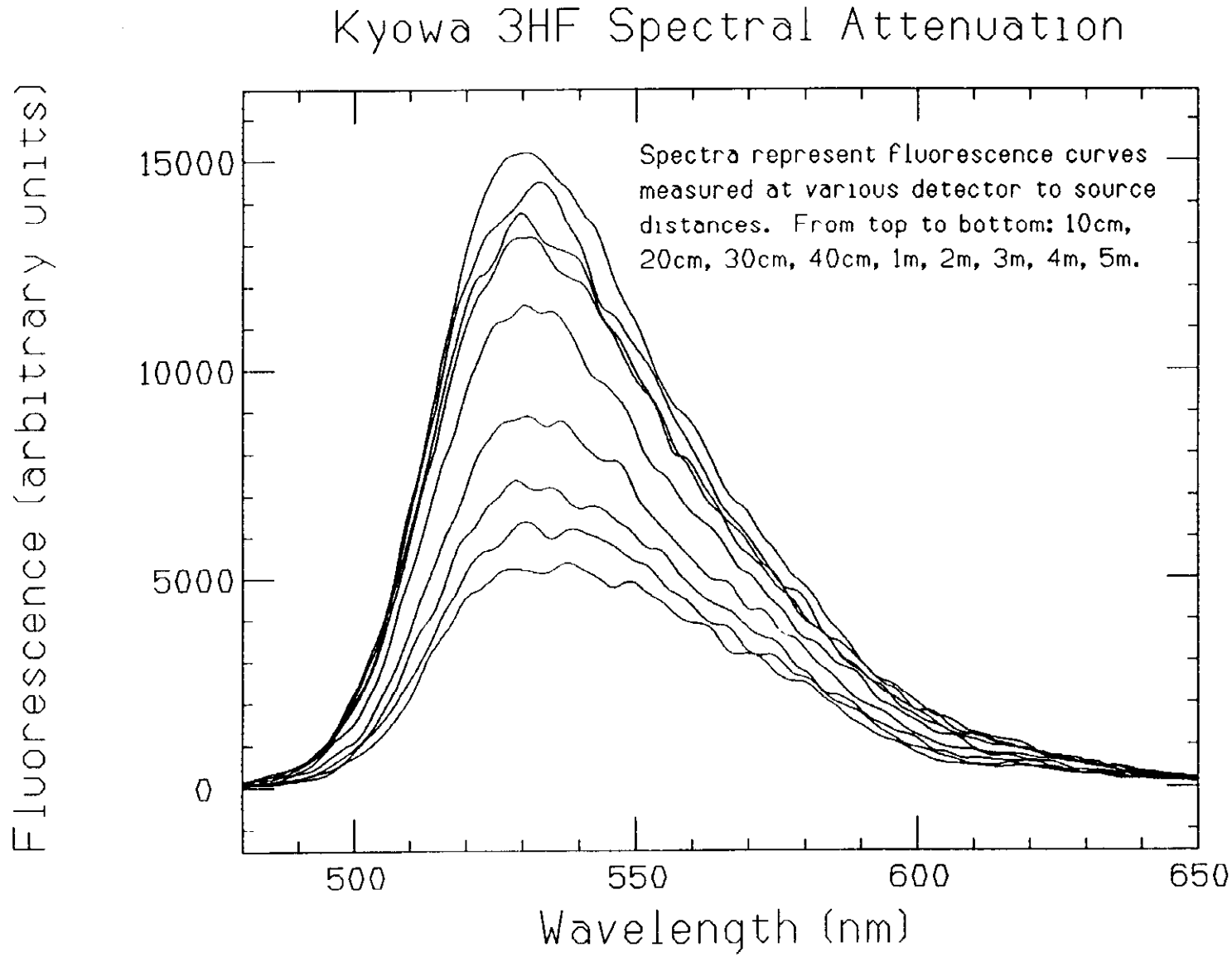
Kyowa 3HF Spectral Attenuation
Fluorescence (arbitrary units)
15000
10000
5000
0
500
550
600
650
Wavelength (nm)
Spectra represent fluorescence curves measured at various detector to source distances. From top to bottom: 10cm, 20cm, 30cm, 40cm, 1m, 2m, 3m, 4m, 5m.

Figure 7

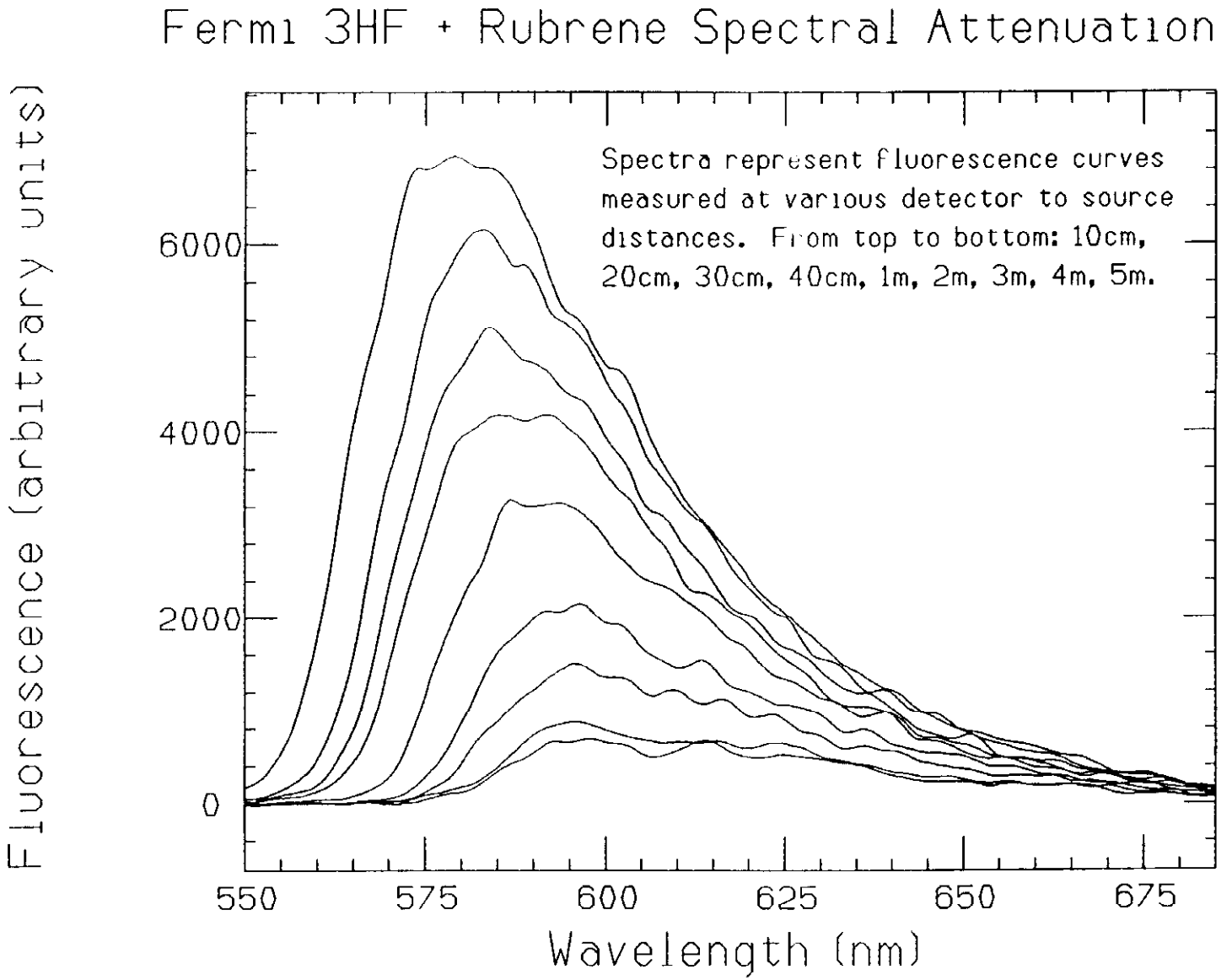
Fermi 3HF + Rubrene Spectral Attenuation
Spectra represent fluorescence curves measured at various detector to source distances. From top to bottom: 10cm, 20cm, 30cm, 40cm, 1m, 2m, 3m, 4m, 5m.
Fluorescence (arbitrary units)
6000
4000
2000
0
550
575
600
625
650
675
Wavelength (nm)

Figure 8

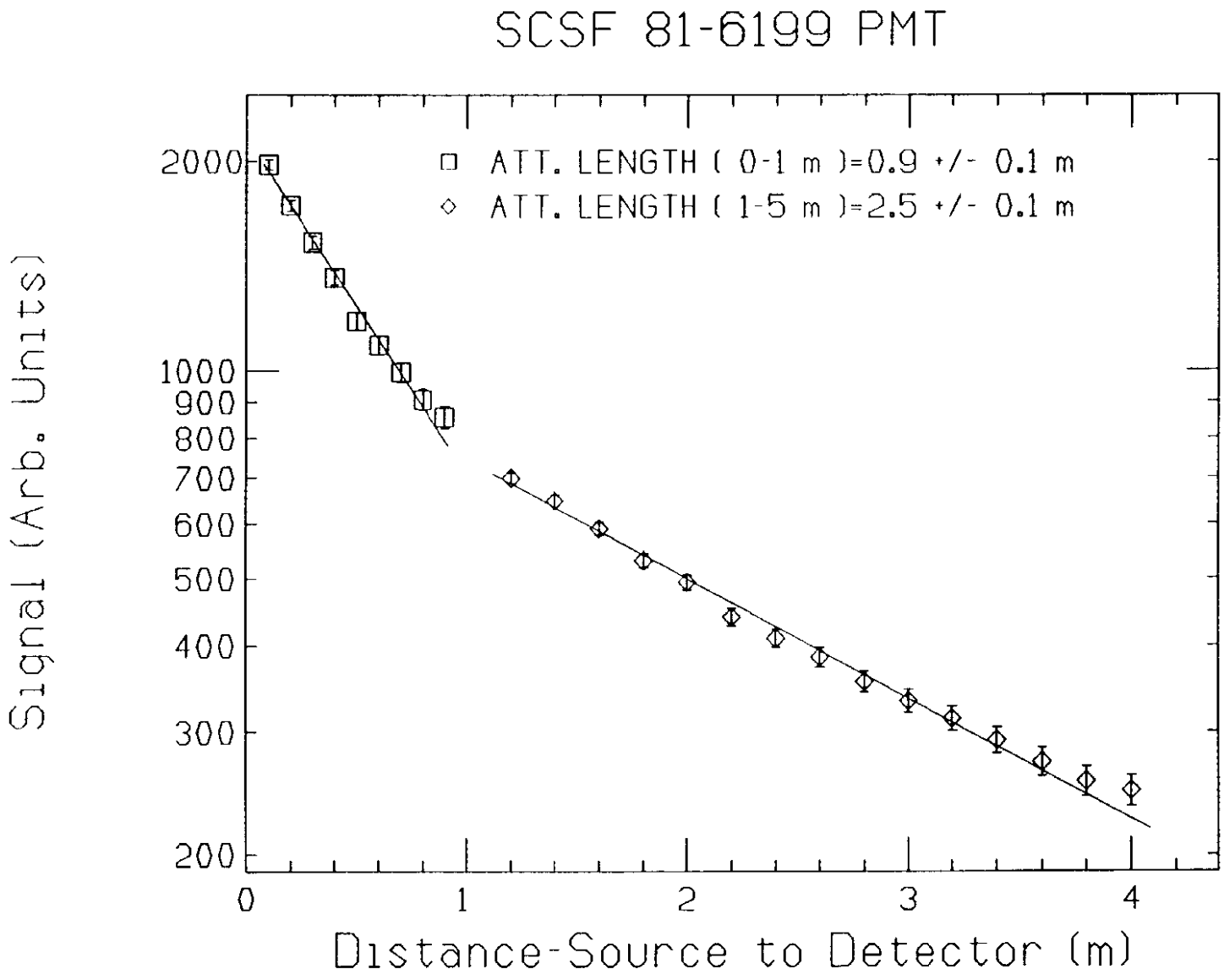
SCSF 81-6199 PMT
ATT. LENGTH (0-1 m)=0.9 +/- 0.1 m
ATT. LENGTH (1-5 m)=2.5 +/- 0.1 m
Signal (Arb. Units)
2000
1000
900
800
700
600
500
400
300
200
0
1
2
3
4
Distance-Source to Detector (m)

Figure 9

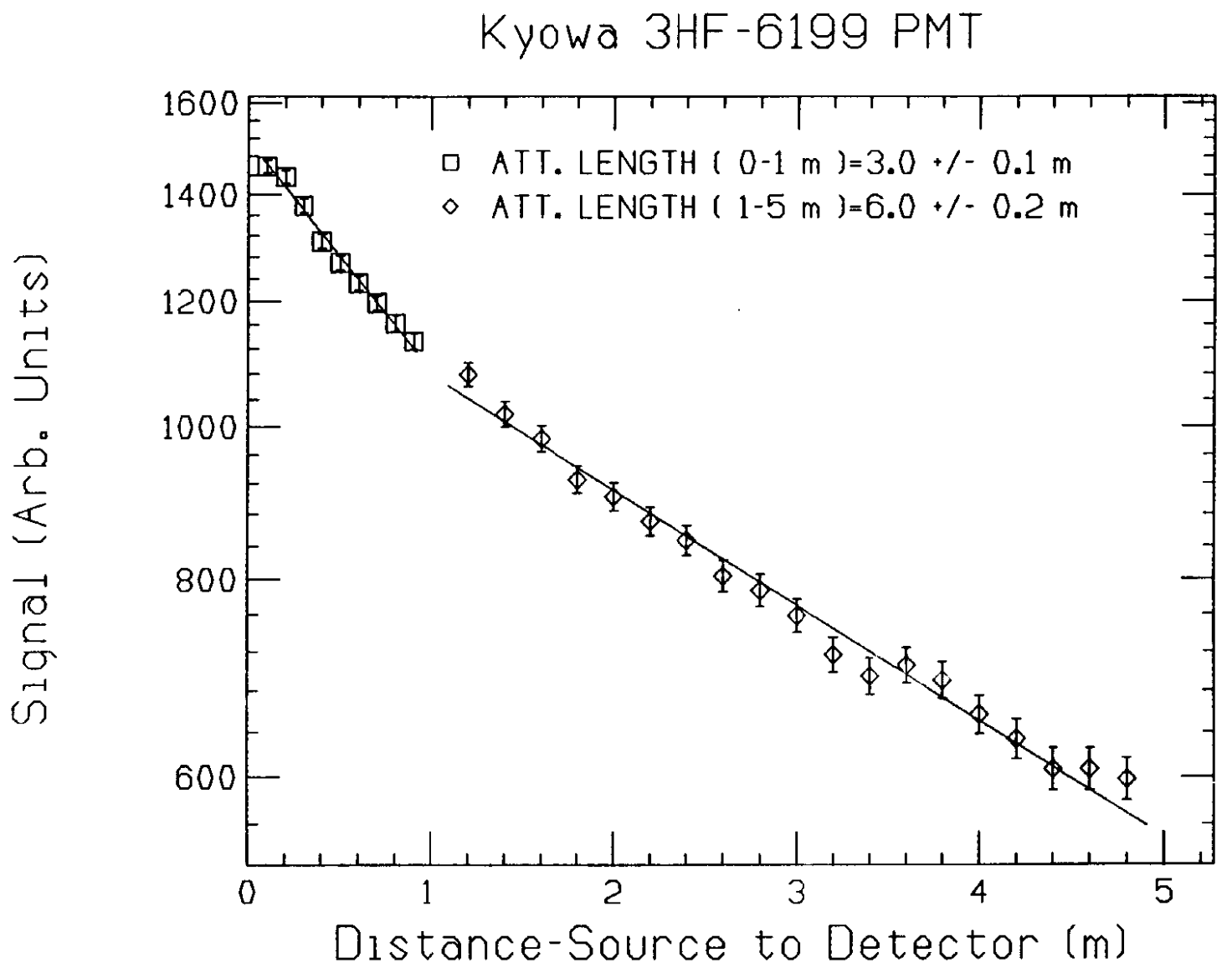
Kyowa 3HF-6199 PMT
ATT. LENGTH (0-1 m)=3.0 +/- 0.1 m
ATT. LENGTH (1-5 m)=6.0 +/- 0.2 m
Signal (Arb. Units)
1600
1400
1200
1000
800
600
0
1
2
3
4
5
Distance-Source to Detector (m)

Figure 10

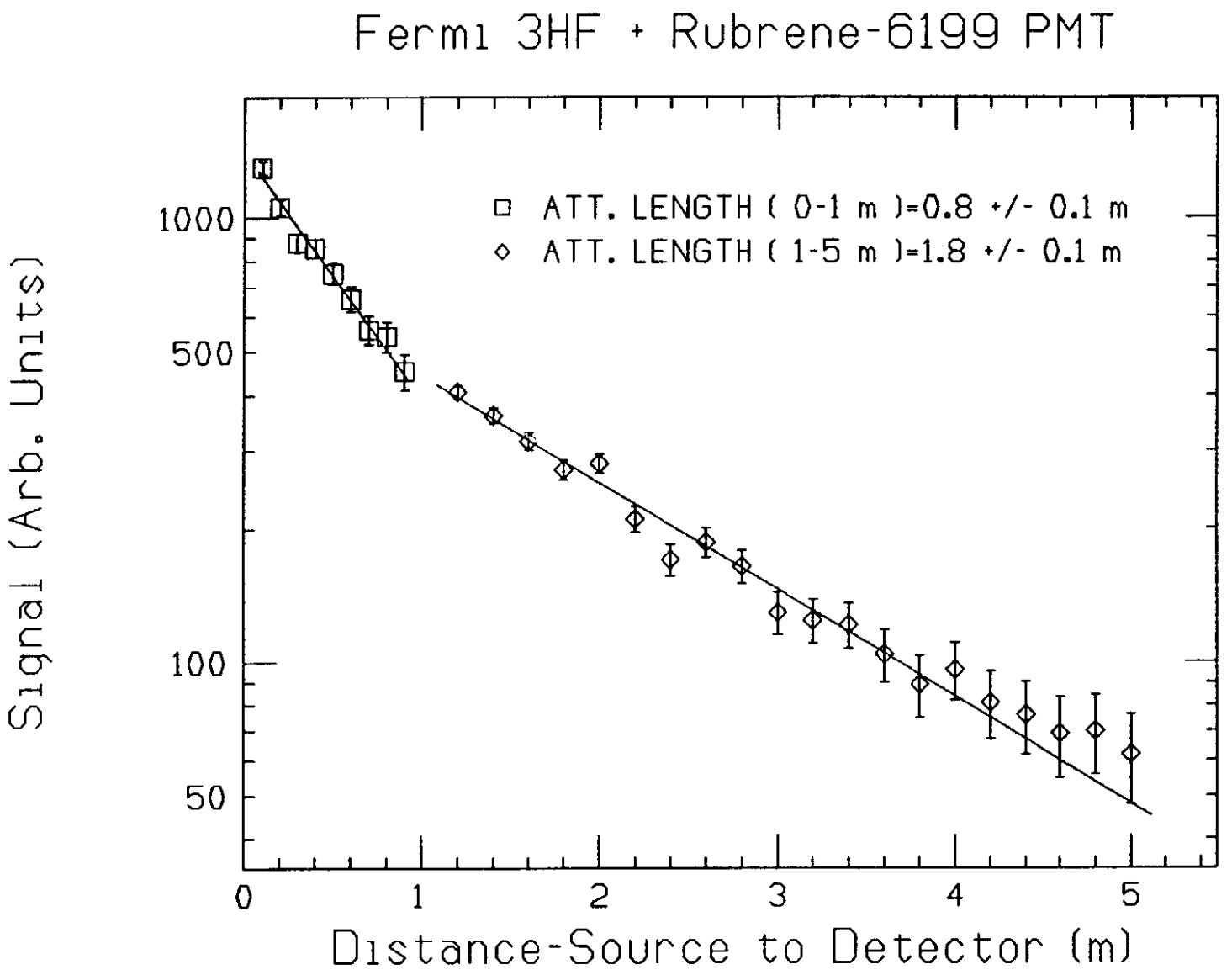
Fermi 3HF + Rubrene-6199 PMT
ATT. LENGTH (0-1 m)=0.8 +/- 0.1 m
ATT. LENGTH (1-5 m)=1.8 +/- 0.1 m
Signal (Arb. Units)
1000
500
100
50
0
1
2
3
4
5
Distance-Source to Detector (m)

Figure 11

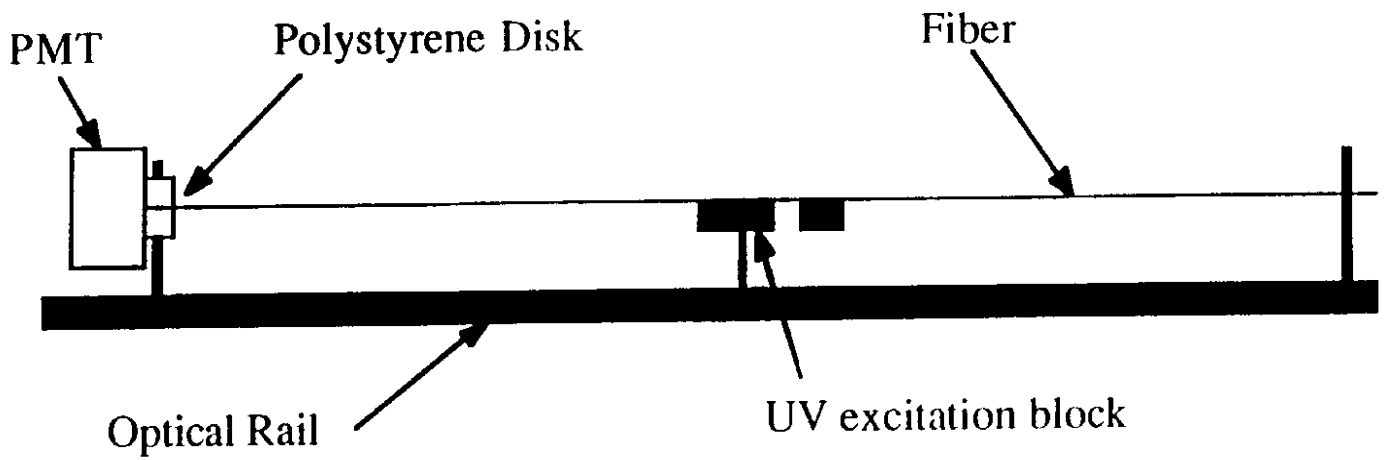

(Not to scale)

Polystyrene disk and fiber detail:

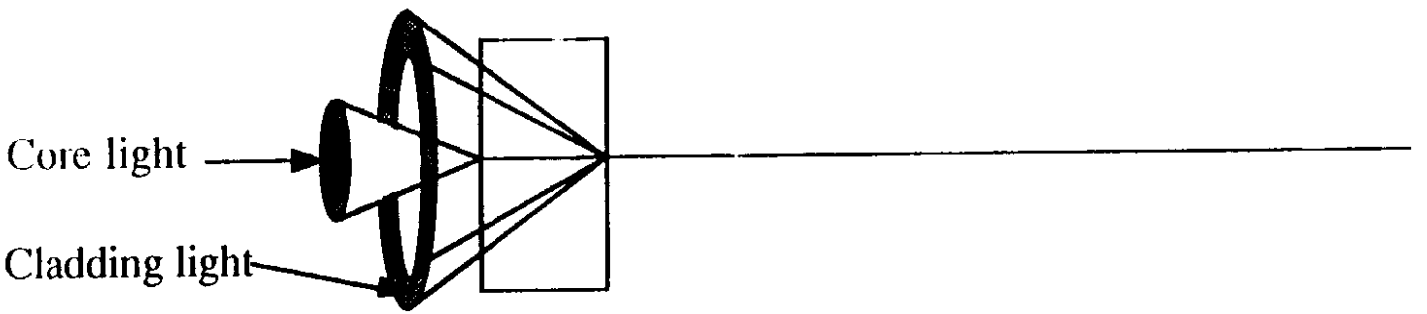

Figure 12

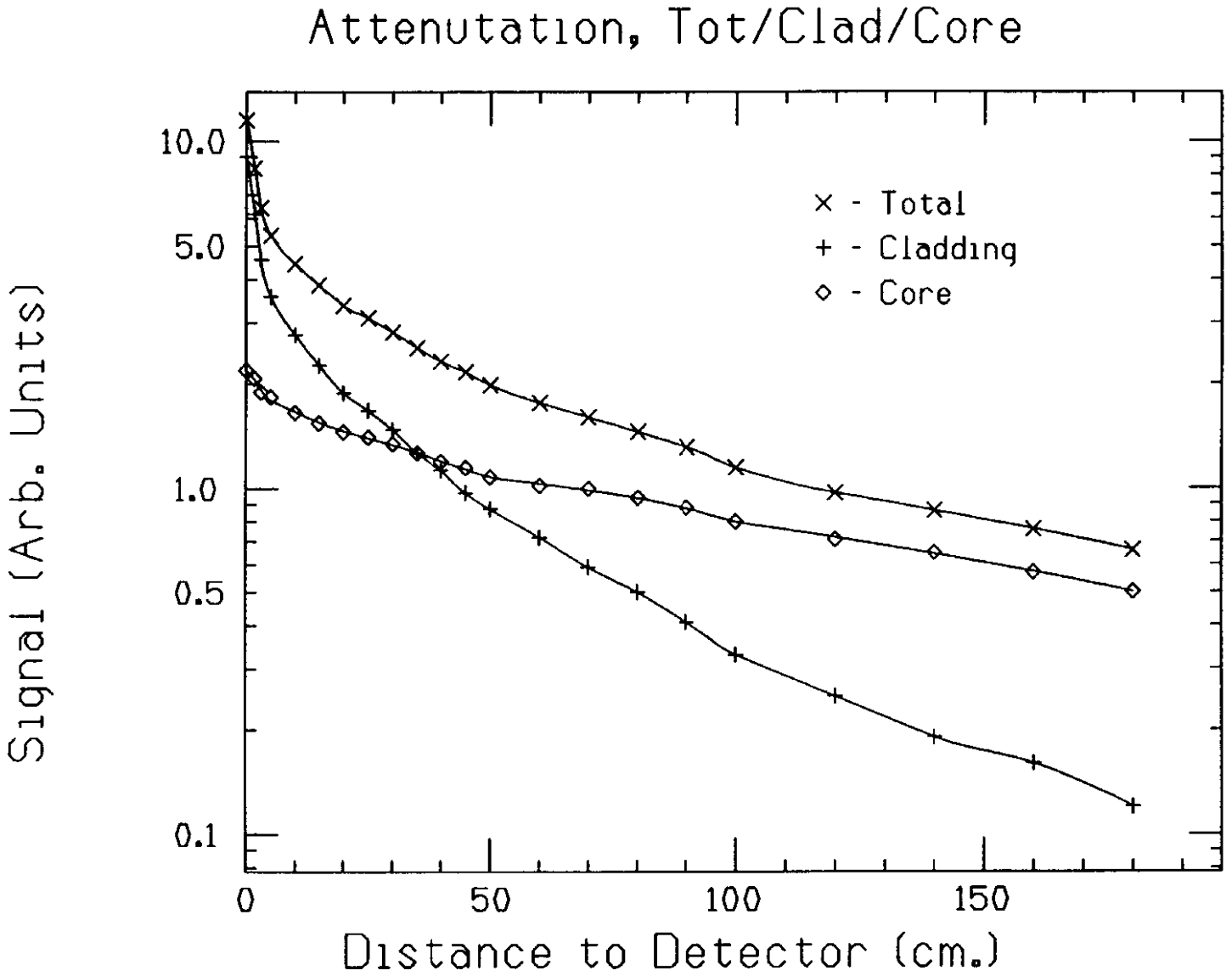
Attenutation, Tot/Clad/Core
10.0
5.0
1.0
0.5
0.1
Signal (Arb. Units)
× - Total
+ - Cladding
◇ - Core
0
50
100
150
Distance to Detector (cm.)

Figure 13

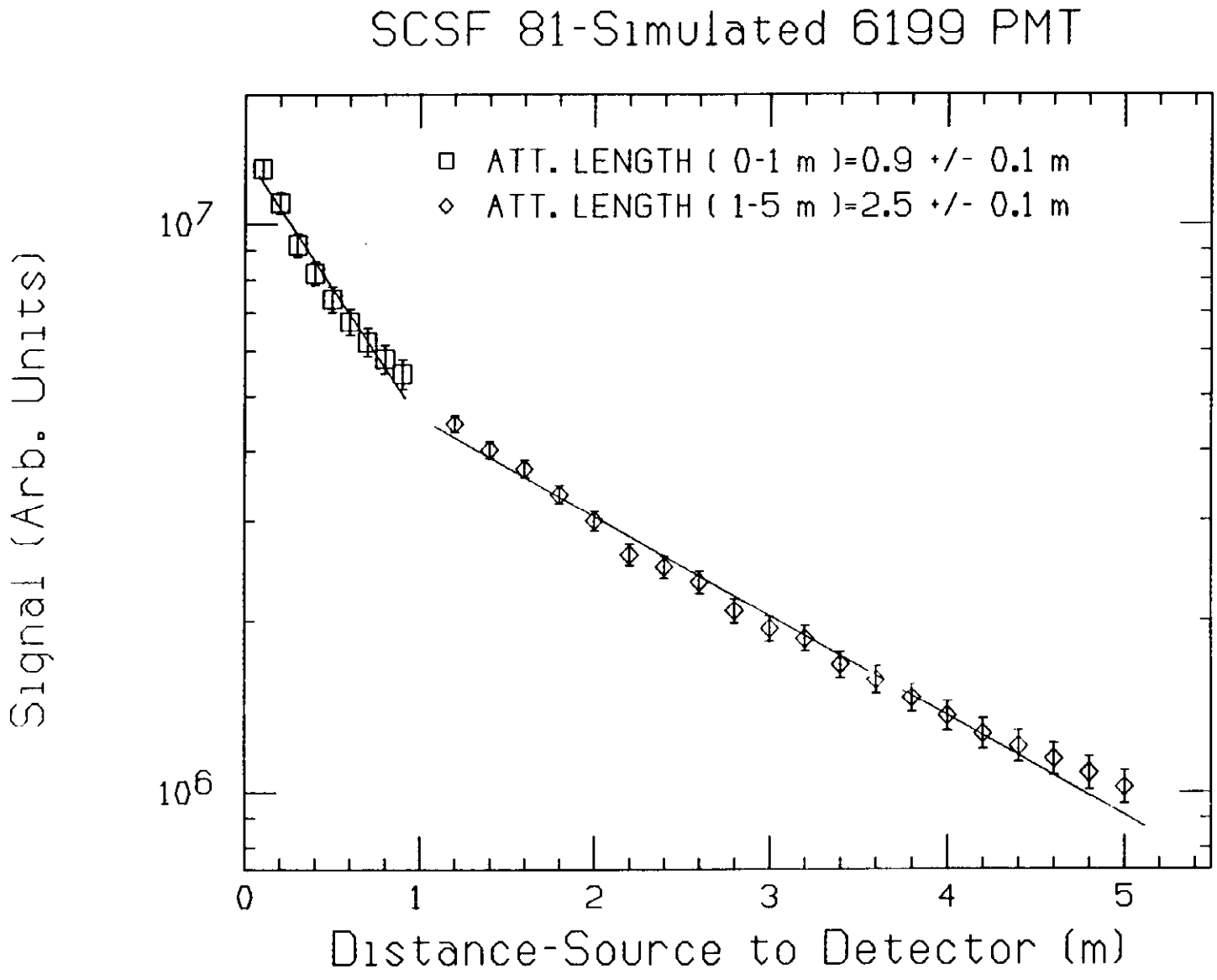
SCSF 81-Simulated 6199 PMT
ATT. LENGTH (0-1 m)=0.9 +/- 0.1 m
ATT. LENGTH (1-5 m)=2.5 +/- 0.1 m
Signal (Arb. Units)
10^7
10^6
0
1
2
3
4
5
Distance-Source to Detector (m)

Figure 14

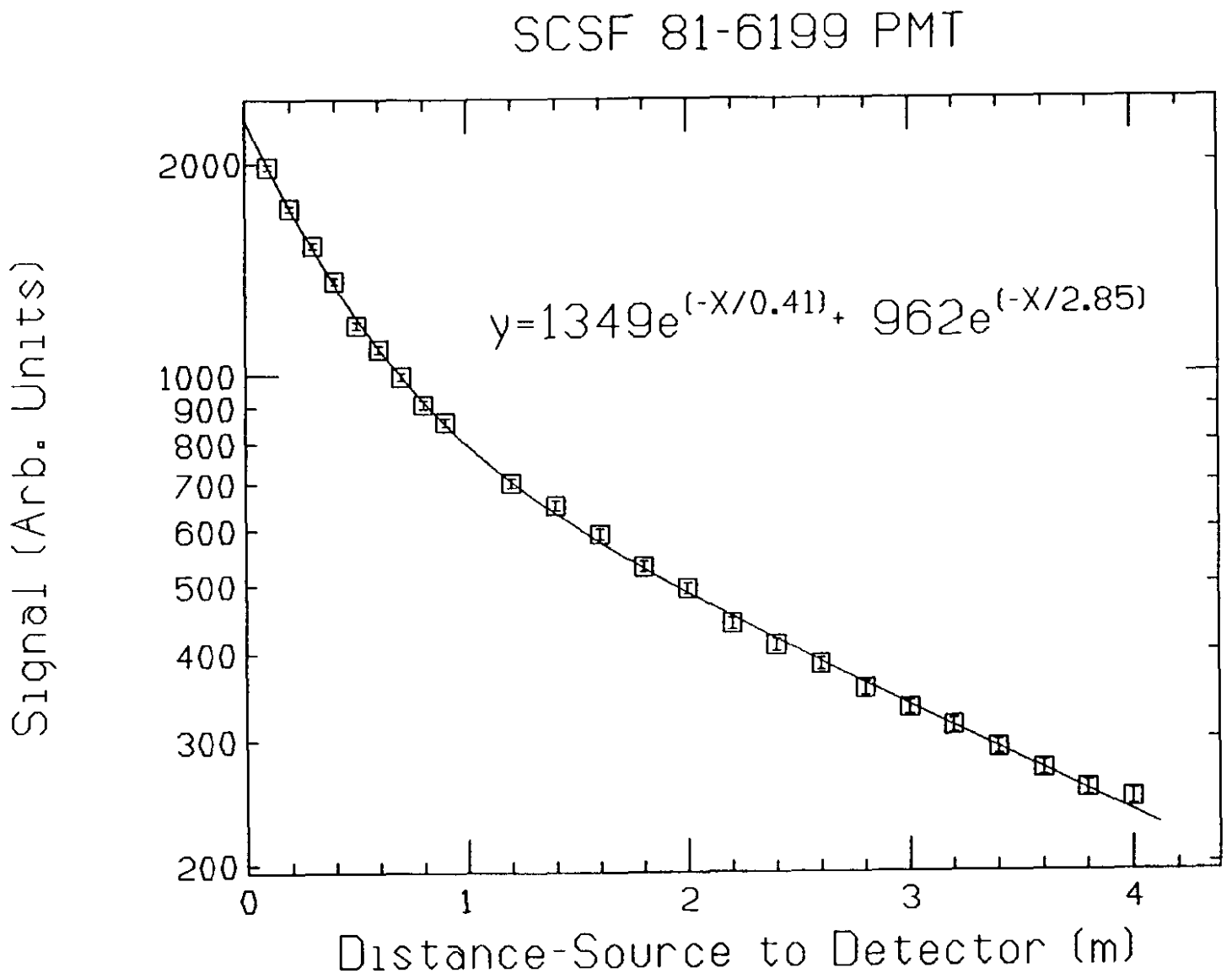
SCSF 81-6199 PMT
y=1349e^(-X/0.41)+ 962e^(-X/2.85)
Signal (Arb. Units)
2000
1000
900
800
700
600
500
400
300
200
0
1
2
3
4
Distance-Source to Detector (m)

Figure 15

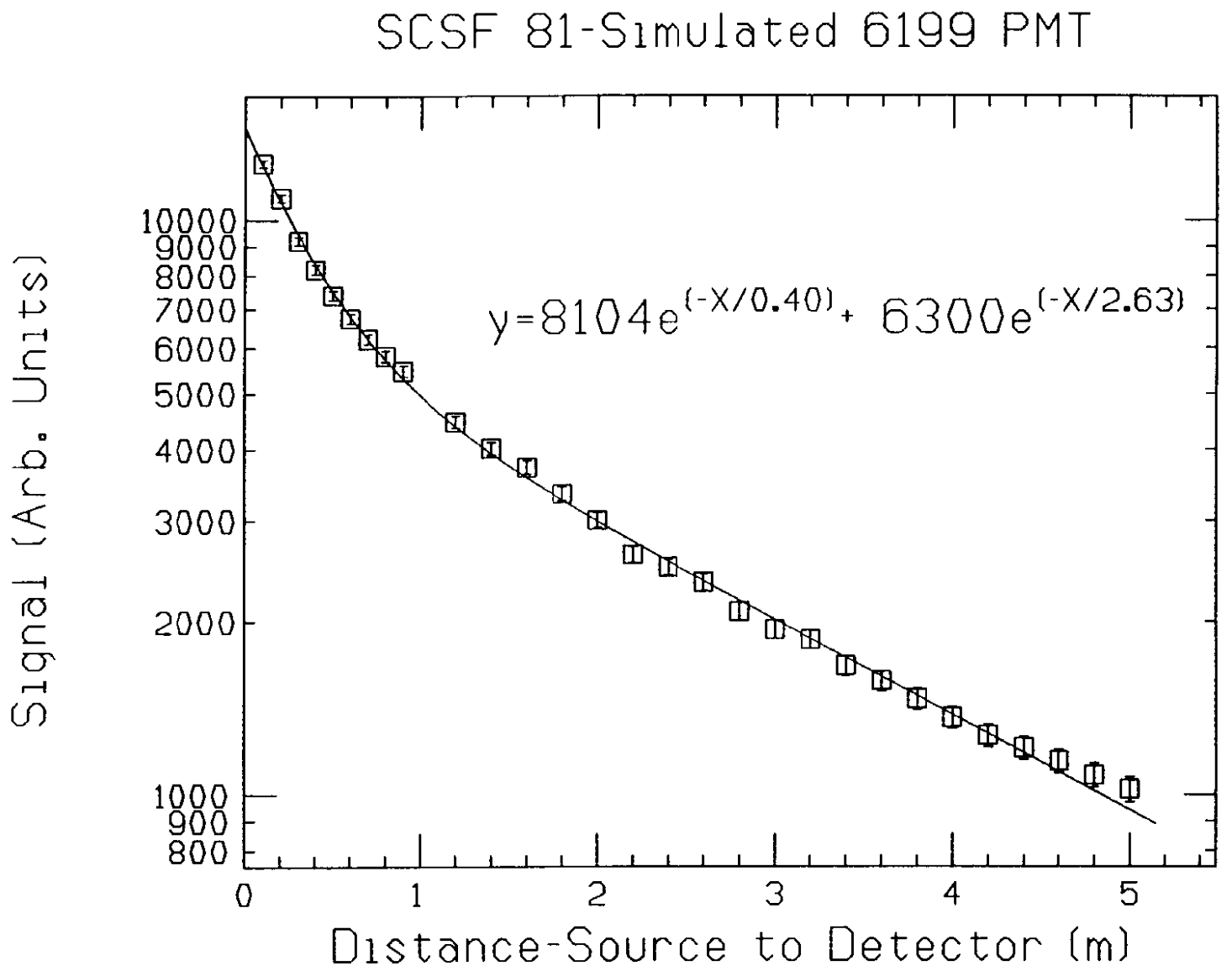
SCSF 81-Simulated 6199 PMT
y=8104e(-X/0.40)+ 6300e(-X/2.63)
Signal (Arb. Units)
10000
9000
8000
7000
6000
5000
4000
3000
2000
1000
900
800
0
1
2
3
4
5
Distance-Source to Detector (m)

Figure 16

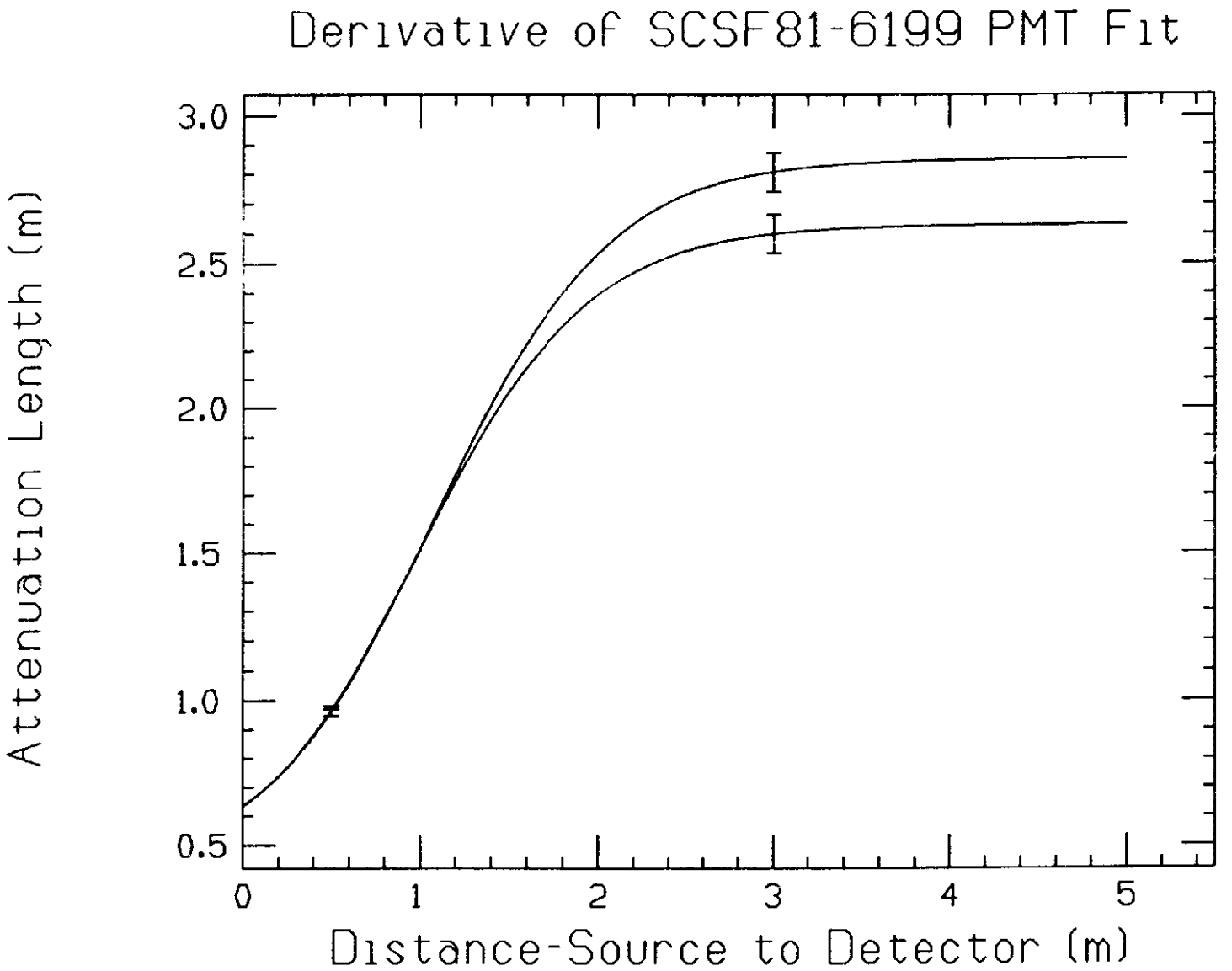
Derivative of SCSF81-6199 PMT Fit
Attenuation Length (m)
3.0
2.5
2.0
1.5
1.0
0.5
0
1
2
3
4
5
Distance-Source to Detector (m)

Figure 17